We are IntechOpen,
the world's leading publisher of
Open Access books
Built by scientists, for scientists

6,900
Open access books available

186,000
International authors and editors

200M
Downloads

Our authors are among the

154
Countries delivered to

TOP 1%
most cited scientists

12.2%
Contributors from top 500 universities

CLARIVATE ANALYTICS

BOOK CITATION INDEX

INDEXED

WEB OF SCIENCE™

Selection of our books indexed in the Book Citation Index
in Web of Science™ Core Collection (BKCI)

Interested in publishing with us?
Contact book.department@intechopen.com

Lightweight Electromagnetic Interference Shielding Materials and Their Mechanisms

Liying Zhang, Shuguang Bi and Ming Liu

Abstract

Motivated by the increase of stress over electromagnetic pollution issues arising from the fast-growing development and need for electronic and electrical devices, the demand for materials with high electromagnetic interference (EMI) shielding performance has become more urgently. Considering the energy consumption in real applications, lightweight EMI shielding materials has been attentive in this field of research. In this chapter, first of all, the EM theory will be briefly discussed. Secondly, the EMI shielding performance and corresponding mechanisms of three categories of lightweight materials, such as polymer-based composites, foams and aerogels, are reviewed. Finally, the summary and conclusions of this field will be addressed.

Keywords: lightweight, EMI shielding, polymer-based composite, foam, aerogel

1. Introduction

Electromagnetic (EM) waves are generated when an electric field comes in contact with a magnetic field. The oscillations of the electric field and the magnetic field are perpendicular to each other and they are also perpendicular to the direction of EM waves propagation. EM waves travel with a constant velocity of 3.0×10^8 m/s in vacuum. Unlike mechanical waves (sound waves) which need a medium to travel, EM waves can travel through anything, such as air, water, a solid material or vacuum. EM radiation refers to the EM waves, propagating through space–time, carrying EM radiant energy [1]. It is a form of energy that is all around us. Human activities like using global positioning system (GPS) device to navigate precise location, heating up a food in a microwave or using X-rays detection by a doctor would be impossible without EM radiation. **Figure 1** shows the EM spectrum used to describe different types of EM energy according to their frequencies (or wavelengths). The EM spectrum ranges from lower energy waves (longer wavelength), like radio waves and microwaves, to higher energy waves (shorter wavelength), like X-rays and gamma rays. As for the radiated emission which is focused on in this chapter, the frequency locates in the radio frequency spectrum (3 KHz–300 GHz).

Electromagnetic interference (EMI) is a disturbance generated by conduction or external radiation that affects an electrical circuit. The interference emission
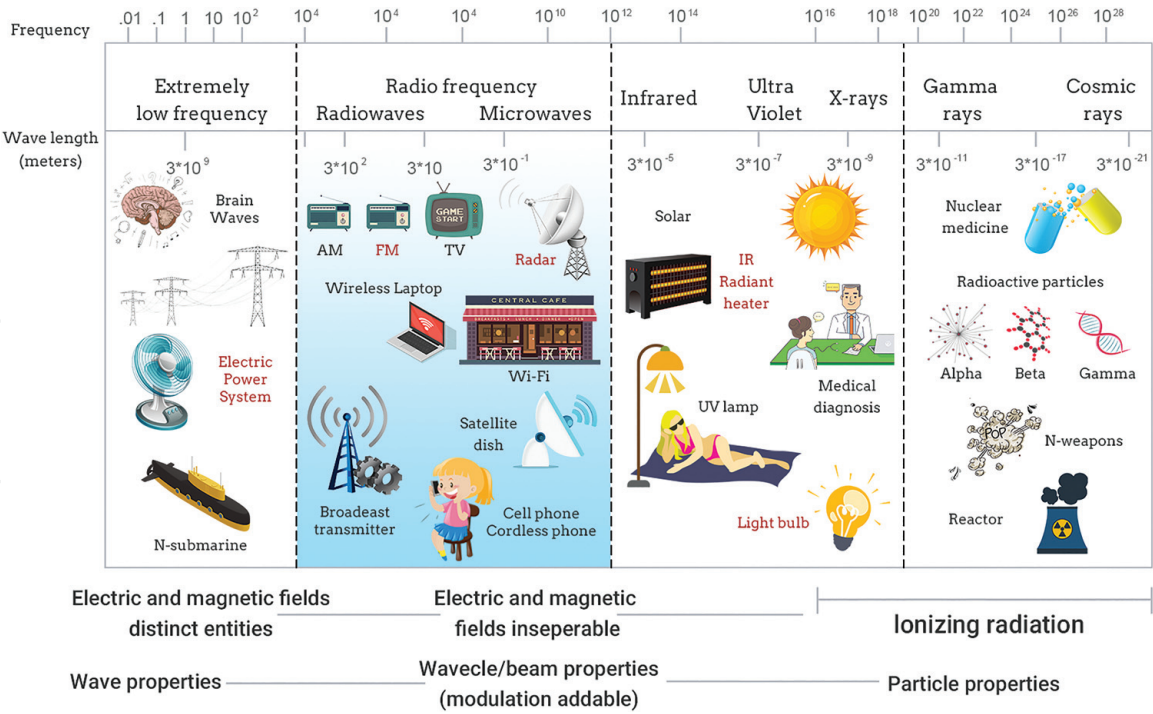
Figure 1.
A diagram of the EM spectrum showing various properties across the range of frequencies and wavelengths.

sources are from the conducted emission (several KHz–30 MHz) to the radiated emission (30 MHz–12 GHz) [2]. The conducted emission is the noise which is internally generated from the poor designed electrical circuit such as electrical cables and power wires. The radiated emission that is externally generated is in the form of transmitting EM waves such as the intended EM radiation from the radio broadcasting antenna and the unintended EM radiation from the high-speed transceivers. While detecting the EMI shielding of the device, it is usually relevant to the radiated emission lonely. The conducted emission is another subject especially for the noise prevention in system level.

EMI is encountered by all of us in our daily life and are expected to face exponential rise in future due to the growing numbers of wireless devices and standards, including cell phones, GPS, Bluetooth, Wi-Fi and near-field communication (NFC). Great effort has been dedicated for the development of EMI shielding materials. EMI shielding can be achieved by prevention of EM waves passing through an electric system either by reflection or by absorption of the incident radiation power. In the past, metals were conveniently used in many occasions. Among them, galvanized steel and aluminum are the most widely used. Copper, nickel, pre-tin plated steel, zinc and silver are also used for some purposes. When the trend in today's electronic devices become faster, smaller and lighter, metals are disadvantageous in weight consideration. Moreover, the EM pollution is not truly eliminated or mitigated since the EM signals are almost completely reflected at the surface of the metal protecting the environment only beyond the shield [3]. Hence, intensive research efforts have been focused on the development of EMI shielding materials that work by tunable reflection and absorption based on novel materials that possess lightness, corrosion resistance, flexibility, easy processing, etc.

This chapter is divided into two sections. In the next section, we will describe the EMI shielding theory in details and the parameters that influence the shielding by reflection and absorption. After that, we introduce three categories of lightweight EMI shielding materials, namely, polymer-based composites, foams and aerogels.

2. EMI shielding theory

The EMI capability of a material is called shielding effectiveness (SE). It is defined in terms of the ratio between the incoming power (P_i) and outgoing power (P_o) of an EM wave as [4]:

$$SE = 10 \log \left(\frac{P_i}{P_0} \right) \tag{1}$$

The unit of EMI SE is given in decibels (dB). According to Eq. (1), how much attenuation is blocked at given SE is given in **Table 1**.

2.1 Far field and near field

According to the distance r between the radiating source and the shield material, an EM wave can be divided into near field wave and far field wave relative to the total wavelength λ of the EM wave. As shown in **Figure 2**, the region within the distance $r > \lambda/2\pi$ is the far field while the distance $r < \lambda/2\pi$ is the near field.

In far field, the EM waves can be regarded as plane waves and EMI should consider both electric field (E) and magnetic field (H) effects. It fulfills the conditions as follows,

$$Z = \frac{|E|}{|H|} \tag{2}$$

$$E \perp H \tag{3}$$

SE (dB)	20	30	40	50	60	70
Attenuation %	99	99.9	99.99	99.999	99.9999	99.9999

Table 1.
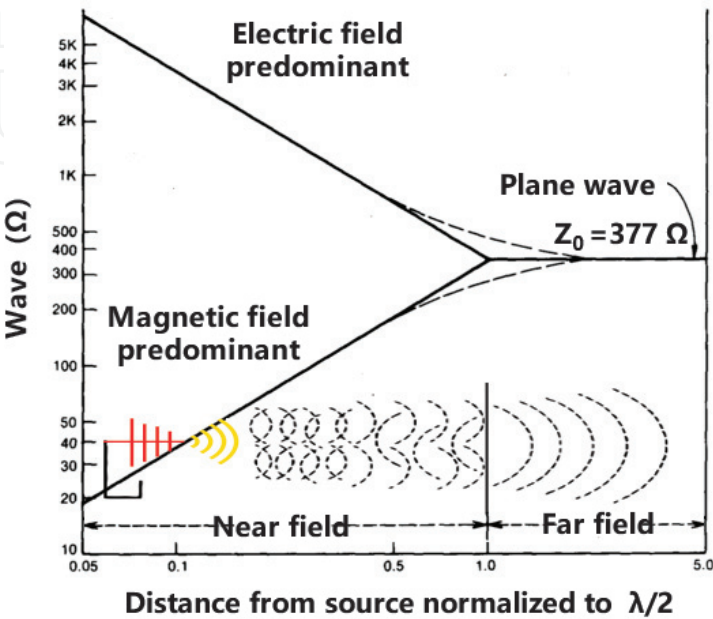*Shielding effectiveness and attenuation %.*

Figure 2.
Wave impedance in far field and near field [5].

where Z is the intrinsic impedance or what is sometimes called wave impedance. $|E|$ and $|H|$ are the electric and magnetic fields' amplitudes, respectively. For air ($\sigma = 0$, $\mu = \mu_0$, $\varepsilon = \varepsilon_0$), the wave impedance ($Z_0$) is always equal to 377 Ω and can be expressed as

$$z_0 = \sqrt{\frac{j\omega\mu}{\sigma + j\omega\varepsilon}} = \sqrt{\frac{j\omega\mu_0}{j\omega\varepsilon_0}} = \sqrt{\frac{\mu_0}{\varepsilon_0}} \approx 377\Omega \quad (4)$$

where σ is the electrical conductivity, μ_r is the relative permeability ($\mu = \mu_0\mu_r$), μ_0 is the permeability of air ($4\pi \times 10^{-7}$ H/m), ε_0 is the permittivity of air (8.85×10^{-12} F/m).

In near field, the wave front is curved instead of planar, so the wave front is not parallel to the surface of the shielding material. In this case, the wave impedance ($|E|/|H|$) is not constant and depends on the distance and the dominant field. For an electrical radiation source, the electrical field dominates. The wave impedance is higher than 377 Ω and decreases as the distance r increases. It can be expressed as [5].

$$z_0 = \frac{1}{2\pi f \varepsilon r} \quad (5)$$

For a magnetic radiation source, the near field is mainly magnetic. The wave impedance is lower than 377 Ω and increases as the distance r increases, it can be expressed as [5].

$$Z_0 = 2\pi f \mu r \quad (6)$$

In this chapter, all the formulations and results are taken based on far field condition because a distance of 48 cm associated with operating at a frequency of 100 MHz is already considered as far field.

2.2 EMI shielding mechanisms for homogeneous shield materials

Figure 3a illustrates the reflection and transmission of an EM wave when it strikes on a shield material. The uniform EM wave with the electric field E_i and magnetic field H_i is normal incident to the material. When the EM wave strikes the left boundary of the material, portions of the EM wave are reflected in the opposite
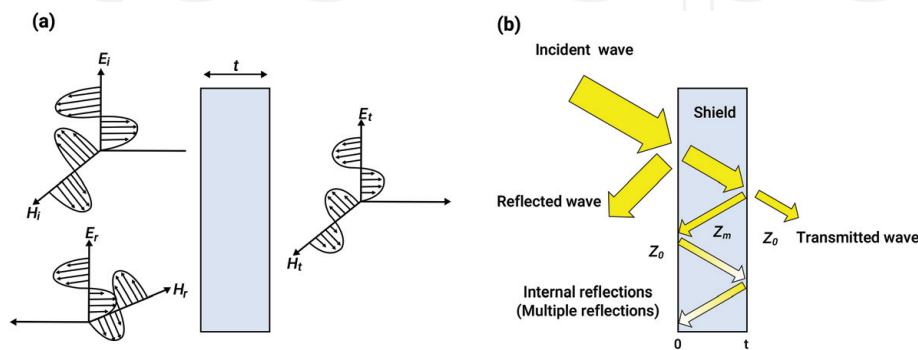

Figure 3.
(a) Schematic illustration of EM plane wave is normal incident to a material with thickness t and (b) schematic illustration of attenuation of an incident EM wave by a shield material (thickness of shield material = t).

direction with the electric field E_r and magnetic field H_r. Other portions of the EM wave are transmitted though the material with the electric field E_t and magnetic field H_t. The electric field SE can be expressed as:

$$SE = 20 \log \left| \frac{E_i}{E_t} \right| \tag{7}$$

The magnetic field SE can be expressed as:

$$SE = 20 \log \left| \frac{H_i}{H_t} \right| \tag{8}$$

Theoretically, the SE of a material is contributed from three mechanisms including reflection, absorption and multiple-reflections., the materials with mobile charge carriers (electrons or holes) can interact with the incoming EM wave to facilitate reflection. Absorption depends on the thickness of the shield materials. It increases with the increase of the thickness of the shield materials. For significant absorption, the shield materials possess electric and/or magnetic dipoles which could then interact with the EM fields. Multiple-reflections is the third shielding mechanism, which operates via the internal reflections within the shield material. Therefore, the overall SE is the sum of all the three terms:

$$SE_{overall} = SE_R + SE_A + SE_{MR} \text{ (dB)} \tag{9}$$

The EMI SE of the material depends on the distance between radiation source and the shielding material. When the radiation source is far from the shielding material, the SE is called as far field SE. In the case of the short distance between radiation source and the shielding material, the SE is called as near field SE.

Figure 3b illustrates three EMI shielding mechanisms in a conductive shield material. When an EM wave strikes the left boundary of the homogenous conductive material, a reflected wave and a transmitted wave will be created at the left external and right external surface, respectively. As the transmitted wave propagates within the shield material, the amplitude of the wave exponentially decreases as a result from absorption, and the energy loss due to the absorption will be dissipated as heat [6]. Once the transmitted wave reaches the internal right surface of the shield (t), a portion of wave continues to transmit from the shield material and a portion will be reflected into the shield material. The portion of internal reflected wave will be re-reflected within the shield material, which represents the multiple-reflections mechanism. The skin effect would affect the effect of multiple-reflections to the overall shielding to a great extent. The depth at which the electric field drops to ($1/e$) of the incident strength is call the skin depth (δ), which is given as follows [7]:

$$\delta = \frac{1}{\sqrt{\pi f \sigma \mu}} \tag{10}$$

where f is frequency (Hz). μ and σ are the magnetic permeability and the electrical conductivity of the shield material, respectively. If the shield is thicker than the skin depth, the multiple-reflections can be ignored. However, the effect of multiple-reflections will be significant as the shield is thinner than the skin depth.

As shown in **Figure 3b**, in case the shield material is a good conductor, $Z_m \ll Z_0$, then [8].

$$SE_R = 20 \log \left| \frac{E_i}{E_t} \right| = 20 \, log \left| \frac{(Z_0 + Z_m)^2}{4 Z_m Z_0} \right| \cong 20 \, log \left| \frac{Z_0}{4 Z_m} \right| \qquad (11)$$

where $Z_m = \sqrt{\frac{j\omega\mu}{\sigma + j\omega\varepsilon}} \cong \sqrt{\frac{j\omega\mu}{\sigma}}$, $Z_0 = \sqrt{\frac{\mu_0}{\varepsilon_0}}$. So SE_{MR} can be expressed as [8].

$$SE_{MR} = 20 \log \left(\frac{1}{4} \sqrt{\frac{\sigma}{\omega \mu_r \varepsilon_0}} \right) = 168 + 10 \log \left(\frac{\sigma_r}{\mu_r f} \right) \qquad (12)$$

where $\omega = 2\pi f$, $\sigma_r = \sigma/\sigma_{Cu}$ is the relative conductivity of the material, it is related to the electrical conductivity of the copper, the electrical conductivity of copper is $\sigma_{Cu} = 5.8 \times 10^7$ S/m. If the shield material possesses electric and/or magnetic dipoles, the attenuation of incident EM wave happens inside the shield material due to the absorption and multiple-reflections, the amplitude of the EM wave declines during wave traveling, and it can be expressed as [8].

$$SE_A = 131.4 t \sqrt{f \mu_r \sigma_r} \qquad (13)$$

$$SE_{MR} = 20 \, log \left| 1 - \left(\frac{Z_0 - Z_m}{Z_0 + Z_m} \right)^2 e^{-2t/\delta} e^{-2j\beta t} \right| \cong 20 \, log \left| 1 - e^{-2t/\delta} e^{-2jt/\delta} \right| \qquad (14)$$

where t is the thickness of the shield material, δ is the skip depth under the operation frequency, β is the propagation constant.

The mechanism of multi-reflections is complicated. For a good conductor material, the multiple-reflection is usually insignificant because most of the incident EM waves are reflected from the external conductive surface of the shield material, and only few penetrated EM waves can be retained for multiple-reflections. The influence is more important for a material that has high permeability and low electrical conductivity. In this case, EM waves can easily penetrate through the external surface of the shield material and most penetrated EM waves are reflected from the second surface of the shield material. The influence is more important in low frequency and is reduced when the frequency gets higher because the ratio between material thickness and skin depth (t/δ) become larger as the frequency increases.

2.3 EMI shielding mechanisms for composites

Composites are made from fillers and matrices with significantly different physical or chemical properties. Hence, EMI shielding mechanisms are more complicated than those for homogeneous shield materials because of the huge surface area available for reflection and multiple-reflections. The EMI SE of composites can be measured experimentally, and it also can be calculated theoretically. The effective relative permittivity ε_{eff} of composites, which is one of the most important parameters in the calculation, can be approximately calculated from the Maxwell Garnett formula as [9]:

$$\varepsilon_{eff} = \varepsilon_e + 3 f \varepsilon_e \frac{\epsilon_i - \epsilon_e}{\varepsilon_i + 2\varepsilon_e - f(\varepsilon_i - \varepsilon_e)} \qquad (15)$$

where ε_e is the relative permittivity of the matrix, ε_i is the relative permittivity of the filler and f is the volume fraction of the filler. If the filler are electrical conductive particles, the relative permittivity ε_i can be expressed as [10]:

$$\varepsilon_i = \varepsilon' - j\varepsilon'' = \varepsilon' - j\frac{\sigma}{\omega\epsilon_0} \qquad (16)$$

where ε' and ε'' are the real and imaginary part of the complex relative permittivity of the filler, respectively. σ is the electrical conductivity of the filler. As shown in **Figure 3b**, the transmission coefficient T can be expressed as [10]:

$$T = \frac{T_1 T_2 e^{-\gamma_m D}}{1 + R_1 R_2 e^{-2\gamma_m D}} \qquad (17)$$

where T_1 and T_2 are the transmission coefficients at the boundary 0 and t, respectively. R_1 and R_2 are the reflection coefficients at the boundary 0 and t, respectively. γ_m is the complex propagation constant. The T_1, T_2, R_1, and R_2 can further be expressed in terms of the impedance Z_0 and Z_m [10]:

$$T_1 = \frac{2Z_m}{Z_m + Z_0} \qquad (18)$$

$$T_2 = \frac{2Z_0}{Z_m + Z_0} \qquad (19)$$

$$R_1 = \frac{Z_m - Z_0}{Z_m + Z_0} \qquad (20)$$

$$R_2 = \frac{Z_0 - Z_m}{Z_m + Z_0} \qquad (21)$$

where Z_0 and Z_m are the impedance of the air and the composite material, respectively. Z_0 can be expressed in Eq. (4) and Z_m can further be expressed as:

$$Z_m = Z_o \sqrt{\frac{\mu_r}{\varepsilon_{eff}}} \qquad (22)$$

The propagation constant γ_m can be expressed as [10]:

$$\gamma_m = j\omega \sqrt{\varepsilon_0 \mu_0 \left(\varepsilon'_{eff} - j\varepsilon''_{eff}\right)} \qquad (23)$$

So, the SE can be calculated in terms of T,

$$SE = -20\, log(|T|) \qquad (24)$$

3. Lightweight EMI shielding materials

When modern electronic devices are designed, high performance EMI shielding materials are highly demanded. In addition, lightweight is one additional important technical requirement for potential applications especially in the areas of automobile and aerospace. In the following section, we will briefly review state-of-the-art research work regarding polymer-based composite, foams and aerogels used for EMI shielding.

3.1 Polymer-based composites

Polymer/conductive fillers composites was seen as a promising advanced EMI shielding materials since the discovery that an insulating polymer would allow the

flow of current through the conductive network stablished by conductive fillers above the percolation threshold. The conductive composite materials preserve the advantages of lightness of polymers, low cost, design flexibility and ease of processing, and the incorporation of conductive fillers circumvent intrinsic nature of polymers being transparent to EM waves through interaction between EM wave and the conductive fillers. Metallic fillers, intrinsically conductive polymers and carbon based electrically conductive fillers are discussed in this section with specific examples. Polymer/magnetic particles composites will also be briefly introduced as magnetic portion is an important component in EM waves that should not be ignored. This section aims to provide a general overview on the preparation of polymer-based EMI shielding materials and the advantages and challenges faced by each category and possible strategies towards enhancing the EMI shielding performances.

3.1.1 Polymer-based composites containing metallic fillers

Metals are typical wave-reflection materials used for EMI shielding purpose owing to their abundance in mobile charge carriers that can interact with the incident EM radiation. Metallic fillers of various physical forms, such as fibers or nanoparticles, were dispersed in the polymer matrix to increase the interaction with the incident EM radiation. Injection-molding provides a direct method to disperse metallic fillers into a polymer matrix. Stainless steel fibers (SSF) introduced into polycarbonate matrix through injection molding shown that EMI SE is heavily dependent on the molding parameters which would give an optimum electrical conductivity [11]. Blended textiles of polyester fibers with SSF showed that the EMI SE is more than 50 dB in the frequencies ranging from 30 MHz to 1.5 GHz [12] (see **Figure 4a**). As shown in **Figure 4b** and **c**, comparison of reflectance, absorbance and transmittance, (identified as reflectivity, absorptivity and transmissibility in **Figure 4**) for SSF and SSF/polyester fiber fabrics as a function of frequency revealed absorption as the dominant EMI shielding mechanism. In the case of SSF/polyester with 10 wt% SSF, EMI shielding by absorption increased from 30 MHz to maximum at 500 MHz and then decreased with the increase in frequency.

The challenges in achieving a good dispersion of metallic fillers and the weight increase make polymer/metallic fillers composites a less popular choice. Much attention was switched to intrinsically conductive polymers (including polyaniline, polyacetylene, and polypyrrole), carbon-based materials (including carbon fibers, carbon black, graphite, graphene, carbon nanotubes and mesoporous carbon), and magnetic materials like carbonyl iron and ferrites (including Fe_3O_4 and α-Fe_2O_3).
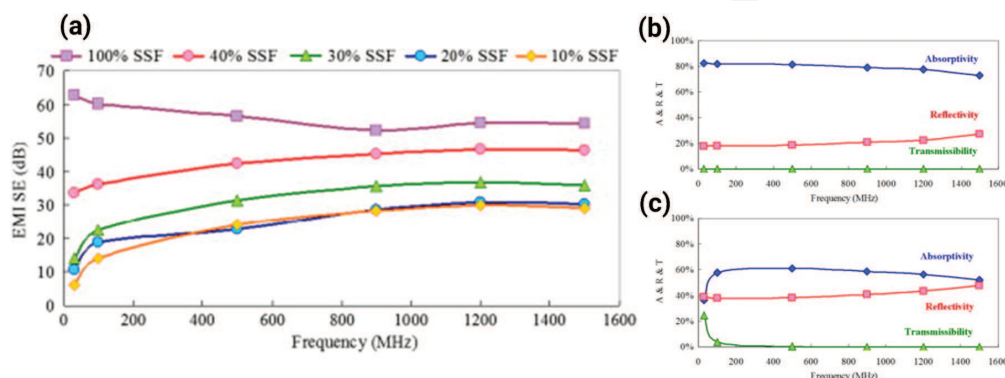

Figure 4.
(a) The EMI SE of the SSF/PET fabric as a function of frequency; (b) reflectivity/absorptivity/transmissibility of SSF fabric and (c) SSF/PET fabric with 10 wt% SSF as a function of frequency [12].

3.1.2 Intrinsically conductive polymers-based composites

Blends of a polymer with an intrinsically conductive polymer results in a composite combining the desired properties of the two components, that is, adequate mechanical properties of the polymer matrix for mechanical support and the electrically conducting component for interaction with the EM radiation. Conducting polymers are conjugated polymers, which on doping exhibit electronic conductivity. Distinctive to metallic fillers, the electrical conductivity of conducting polymers arises from the polymer molecular structure. Alteration of parameters such as chain size, doping level, dopant type and the synthesis route directly affect the molecular structure, hence the EMI shielding properties of the material.

Among the available conducting polymers, polypyrrole (PPY) and polyaniline (PANI) are the most widely used conductive fillers for EMI shielding purposes. PPY is known to possess high conductivity, easy synthesis, good environmental stability and less toxicological problem. Chemical and electrochemical polymerization of PPY on a polyethylene terephthalate (PET) fabric is given as an example for electrically conducting composite. Pyrrole was first dissolved in an aqueous solution containing 10 wt% polyvinyl alcohol (PVA) and sprayed on the PET fabric before subject to electrochemical polymerization at room temperature under a constant current density. The resultant PPY coated PET fabric was shown to exhibit EMI SE about 36 dB over a wide frequency range up to 1.5 GHz [13].

PANI was studied extensively for its various structures, unique doping mechanism, excellent physical and chemical properties, stability, and the readily obtainable raw materials. Lakshmi et al. [14] prepared PANI-PU composite film by adding aniline to polyurethane (PU) solution in tetrahydrofuran (THF). Doping of composites was done by adding camphor sulfonic acid to the composite solution. The EMI SE of the PU-PANI film was found to increase with thickness and the frequency specific material is ideal for shielding at 2.2 and 8.8 GHz.

Other intrinsically conducting polymers, such as poly(p-phenylene-vinylene) [15, 16] and poly(3-octylthiophene) [17], were also investigated for EMI shielding applications, but too much lesser extent, mainly due to the unsatisfactory performance and complex processing procedures involved.

In general, the EMI shielding performance arises by the addition of conductive polymer consequently dominated by reflection mechanism due to the increase of the level of impedance mismatch with air. One obvious advantage of such polymer-polymer system is the lightweight being preserved, also there is no issue on substrate flexibility as those associated with metallic or carbon-based fillers. However, the main drawbacks of such composites include (1) poor mechanical properties of the most of the intrinsically conducting polymers require a matrix material for structural support; (2) the insoluble and infusible characteristics caused conducting polymers to exhibit poor processability and (3) high filler (conducting polymer) level is usually needed for acceptable performances.

3.1.3 Polymer-based composites containing carbon-based fillers

Similar to metallic fillers, carbon-based fillers come in various shapes and aspect ratios. Carbon black (CB), including graphite and CB, is the generic name given to small particle size carbon pigments which are formed in the gas phase by thermal decomposition of hydrocarbons [18]. Carbon fibers (CFs) are 1D carbon structure of diameter generally lies between 50 and 200 nm and aspect ratios around 250 and 2000, largely produced by chemical vaporization of hydrocarbon [19, 20]. Carbon nanotubes (CNTs) can be considered as rolled-up hollow cylinders of graphene sheets of very high aspect ratio due to the small diameter, constituted of a single

hollow cylinder, that is, single-walled carbon nanotubes (SWCNTs) or of a collection of graphene concentric cylinders, that is, multi-walled carbon nanotubes (MWCNTs) [21, 22]. Graphene sheet (GS), an atomically thick two-dimensional structure, exhibited excellent mechanical, thermal and electrical properties [23]. Both CNTs and graphene offer substantial advantages over conventional carbon fillers and the percolation threshold can be achieved by both at very low content if properly dispersed.

In general, carbon fillers with high aspect ratio are generally more effective in imparting electrical conductivities to a polymer matrix, hence it is no surprise to observe the highest SE from fillers with the highest aspect ratio, that is, SWCNTs > MWCNTs > CNFs > CB when the volume fraction of the fillers is the same. The different methods of fillers dispersion and various carbon filler surface modification methods were comprehensively reviewed in the published paper and will not be discussed in detail here [3, 24]. The EMI shielding performance of the polymer/carbon-fillers composites can also be found in Ref. [3, 7, 24, 25].

3.1.4 Polymer-based composites containing magnetic particles composites

A binary or even ternary component consists of two or more types of the fillers provide an effective way to bypass the inherent shortcomings of a single-filler composite. The incorporation of magnetic components will supplement the attenuation properties of a carbon-based EMI shielding material.

Physical blending or deposition of metallic particles within a polymer blend or structure is the most direct way of incorporation a third element, however, such method faces the problem of uniform dispersion and deposition at the bottom layers due to the higher density of metallic particles. Electroless plating of metals on carbon substrates provides a neat way of incorporating metal components uniformly into a system without excessive weight addition. Works by Kim et al. [26] and Yim et al. [27] dispersed nickel coated MWCNT through electroless plating in epoxy and high-density polyethylene, respectively. **Figure 5a** gives an illustration of
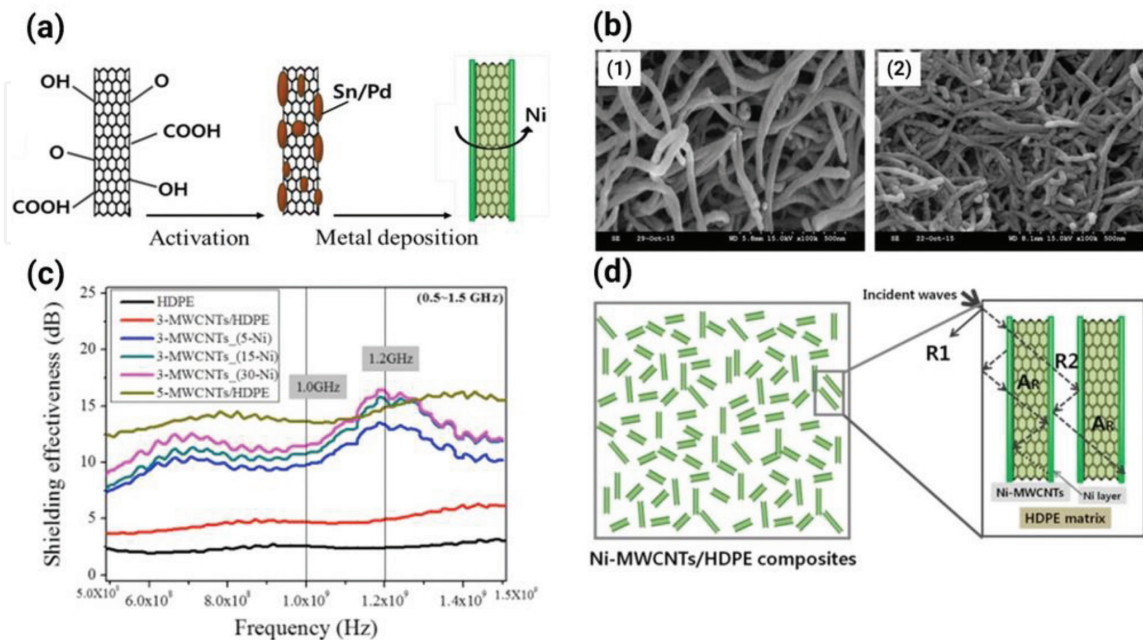

Figure 5.
(a) Schematic diagram of the electroless Ni-plating process; (b) SEM images of (1) pristine MWCNTs and (2) Ni-coated MWCNTs, respectively; (c) comparison of the EMI SE of MWCNTs/HDPE and Ni-MWCNTs/ HDPE and (d) the proposed shielding mechanism of Ni-MWCNTs/HDPE [27].

the nickel coated MWCNTs. It is apparent that the nickel coated MWCNTs appeared rougher comparing to the pristine ones due to the presence of nickel particles as shown **Figure 5b**. Yim achieved 140% (at 1 GHz, **Figure 5c**) in enhancement of the EMI SE compared to the pristine MWCNT/polymer composites. The enhancement was attributed to the increased surface conductivity. **Figure 5d** shows the proposed shielding mechanism of Ni-MWCNTs/HDPE. EM wave was firstly reflected at the composite surfaces upon reaching the surface of the composite. When the penetrated EM wave meets the nickel layer on the MWCNTs, the metallic layer functioned as EM absorbable or reflective fillers. It is evident that the EMI absorbing nature of the metallic layer can be used as an effective additional shielding material despite the small amount present in the systems.

3.2 Foams and aerogels used in EMI shielding

In view of the rigid index of fuel-economy in the applications of automobile and aerospace, lightweight EMI shielding materials with the combination of reduced density and high EMI SE are much preferred. In this section, we aim to provide a general overview on the preparation of foam and aerogel materials used in EMI shielding and the advantages and challenges faced by each category and possible strategies towards enhancing their EMI shielding performances. The specific EMI SE, defined as the ratio of the EMI SE to the density (SSE) or both density and thickness (SSE/t), is a more appropriate criterion to compare the EMI shielding performance with those of other typical materials for the applications where lightweight is required.

3.2.1 Polymer-based composite foams

Conductive polymer-based composites foams offer significant reduction in weight, while the pores decrease the real part of the permittivity, accordingly reducing the reflection at the material surface. The porous structure enhances the energy absorption through wave scattering in the walls of the pores. Electrically conductive fillers, including CNFs, CNTs and graphene sheets, are commonly used to form a desirable conducting network within the inherently insulating polymer foam matrix. Yang et al. [28] first reported CNFs reinforced polystyrene (PS) composite foam as a conductive foam for EMI shielding application. The EMI SE of PS/CNFs foam containing 1 wt% CNFs was less than 1 dB, upon increasing CNFs content to 15 wt%, EMI SE increased to 19 dB. Following this work, the authors reported PS/CNTs composite foam with varying CNTs contents from 0 to 7 wt% [4]. The PS/CNTs composite foam achieved a higher EMI SE of above 10 dB compared to 3 dB for the PS/CNFs composite foam at the same filler content of 3 wt%. The difference in the results originated from the remarkable electrical and structural properties of CNTs, such as larger aspect ratio, smaller diameter, higher electrical conductivity and strength, compared to CNFs.

3.2.2 Syntactic foams

Syntactic foam, filling hollow spheres in a matrix, is a kind of lightweight composite materials. The approaches to enhance the EMI SE of syntactic foams include (i) hollow particles made of a conductive material; (ii) coating a conductive layer onto the surface of hollow particles and (iii) adding a second conductive filler in syntactic foam matrix.

Zhang et al. [29] added a second conductive filler, (CNFs, chopped carbon fiber (CCF), and long carbon fiber (LCF)), into syntactic foams containing conductive

Filler content (vol%)	CNF Aspect ratio: 500–1700	CCF Aspect ratio: 6–50	LCF Aspect ratio: 150–750
0.5	5.2	2.2	2.8
1.0	11.3	3.4	4.4
1.5	16.4	3.7	6.5
2.0	24.9	4.3	7.5

Table 2.
Comparison of the EMI SE (dB) of CNF, CCF, and LCF reinforced syntactic foam.

hollow carbon microspheres (HCMs). The EMI SE values of used syntactic foams at the same filler content were compared, as shown as **Table 2**. The results showed that CNFs is more effective in providing EMI shielding compared to CCF and LCF due to the larger aspect ratio of CNFs.

Zhang et al. [30] also demonstrated the effect of functionalization of HCMs on the EMI SE of the epoxy-HCMs syntactic foam. HCMs were coated with polydopamine (PDA) via the self-polymerization of dopamine. The PDA coating promotes dispersion and served as a reducing agent to deposit silver (Ag) particles on the surface of HCMs as illustrated in **Figure 6a**. The average EMI SE of the epoxy-HCMs syntactic foam containing Ag-PDA-HCMs with 28.5 and 30.5 wt% of silver in the X-band achieved 49.5 and 60.2 dB, respectively as shown in **Figure 6b**. The SSE reached up to 46.3 dB cm^3/g, demonstrating the prospect of epoxy/Ag-PDA-HCMs syntactic foam as a lightweight high-performance EMI shielding material. The corresponding EMI shielding mechanism of this syntactic foam was analyzed by comparing the values of reflectance (R), absorptance (A), and
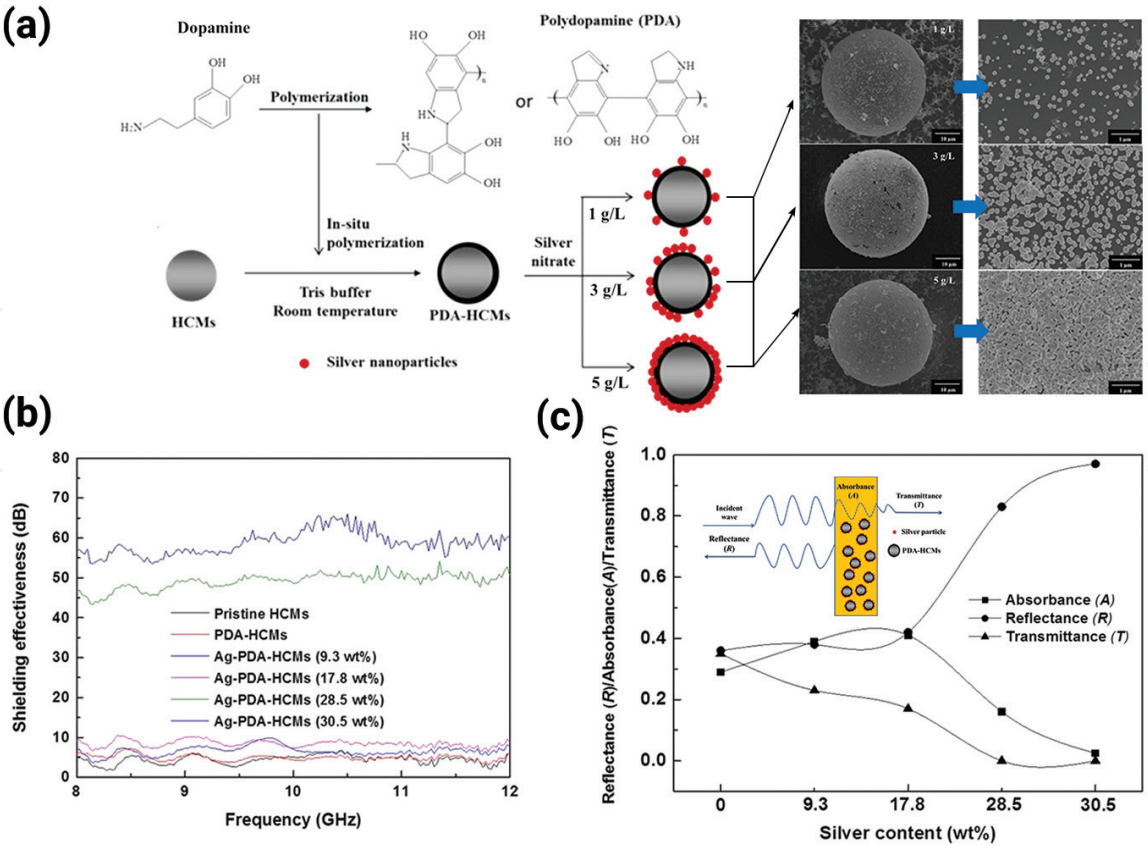

Figure 6.
(a) Schematic illustration of the procedure for preparation of PDA-HCMs and Ag-PDA-HCMs; (b) EMI SE in the frequency range from 8 to 12 GHz for syntactic foam containing pristine HCMs and Ag-PDA-HCMs with different silver contents; and (c) reflectance (R), absorbance (A), and transmittance (T) of EM radiation over syntactic foams containing Ag-PDA-HCMs with different silver content at 10 GHz [30].

transmittance (*T*) in **Figure 6c**. The specimens were both reflective and absorptive towards EM radiation at silver content less than 17.8 wt%. The contribution of reflection (0.83) towards EMI SE surpassed that from absorption (0.16) when silver content increased to 28.5%. The dense and thick electrically conductive silver formed due to further increasing the silver content to 30.5 wt% increased the *R* to 0.97 and resultant in reflection as the dominant shielding mechanism.

Xu et al. [31] fabricated syntactic foams ("hybridized epoxy composite foams" according to authors) through impregnating expandable epoxy/MWCNT/micro-sphere blends into a preformed, highly porous, and 3D silver-coated melamine foam (SF) sponge. The highly conductive SF resolved the problem of the foam reduction of high filled epoxy blends and provided channels for rapid electron transport. MWCNTs were used to offset the loss of conductive pathways due to the crystal defects in the silver layer and the insulating epoxy resin. As a result, the EMI SE of 68.1 dB was achieved with only 2 wt% of MWCNTs and 3.7 wt% of silver due to the synergy of the MWCNT and SF.

3.2.3 Carbon foams

Carbon foam is a class of three-dimensional (3D) architecture consisting of a sponge-like interconnected network of porous carbon. Carbon foams have been wildly used as candidates for realistic EMI shielding applications due to their excellent properties, such as low density, resistance to chemical corrosion, high thermal and electrical conductivity, and high temperature resistance.

Zhang et al. [32] prepared a novel ultralight (0.15 g/cm^3) carbon foam by direct carbonization of phthalonitrile (PN)-based polymer foam, as shown in **Figure 7a**. High EMI SE of ~ 51.2 dB (see **Figure 7b**, C1000 was labeled as the carbonization of 1000°C) was contributed by the high graphitic carbonaceous species and the intrinsic nitrogen-containing structure. The carbon foams showed the best SSE of 341.1 dB cm^3/g so far when mechanical property was considered. The carbon foam developed by Zhang provides an excellent low-density and high-performance EMI shielding material for use in areas where mechanical integrity is desired.

3.2.4 CNTs/graphene foams

The EMI SE of carbon foams was closely related to the char yield of polymer precursors and the demanding carbonization conditions. Therefore, a new kind of filler-free lightweight EMI shielding material, is in demand, which can be prepared without the stringent processing conditions. In view of the lightweight requirement, assembling one dimensional (1D) CNTs and two-dimensional (2D) graphene sheets into three dimensional (3D) macroscopic porous structures (e.g., sponges, foams and aerogels) emerged as an efficient approach.
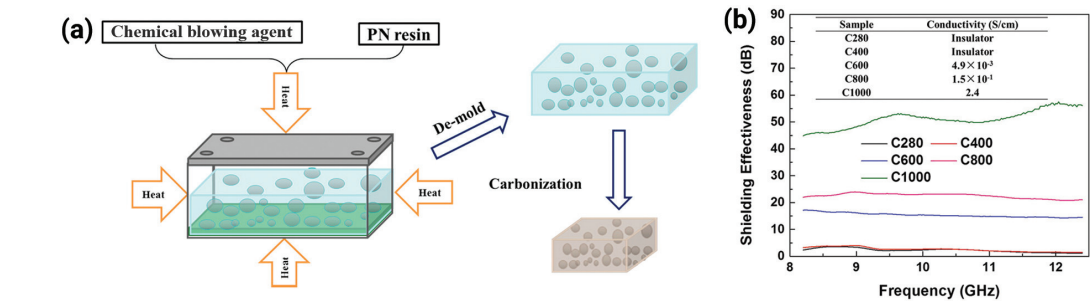

Figure 7.
(a) Schematic representation of the preparation of PN-based carbon foams and (b) EMI SE of carbon foams [32].

Lu et al. [33] synthesized a flexible CNTs sponge with a density of 10.0 mg/cm^3 via chemical vapor deposition (CVD) process, composed of self-assembled and interconnected CNT skeletons. The freestanding CNTs sponge showed the high EMI SE and SSE of 54.8 dB and 5480 dB cm^3/g in X-band, respectively. After composited with polydimethylsiloxane (PDMS) by directly infiltrating method, the CNT/PDMS composites still exhibited excellent EMI SE (46.3 dB) at the thickness of 2.0 mm, while the CNT loading content was less than 1.0 wt%.

Surface modification is employed to increase the EMI shielding ability of graphene foams. Zhang et al. [34] prepared surfaced modified 3D graphene foams via self-polymerization of dopamine with a subsequent foaming process, as shown in **Figure 8a**. The polydopamine (PDA) served as a nitrogen doping source and an enhancement tool to achieve higher extent of reduction of the graphene through providing wider pathways and larger accessible surface areas. The enhanced reduction of graphene sheets and the polarization effects introduced by PDA decoration compensated the negative effect of the barrier posed by PDA. As a result, the resultant EMI SE showed 15% improvement compared to PDA-free graphene foam as shown in **Figure 8b**. Wu et al. [35] also fabricated an ultralight, high performance EMI shielding graphene foam (GF)/poly(3,4-ethylenedioxythiophene):poly(styrene sulfonate) (PEDOT:PSS) composites by drop coating of PEDOT:PSS on the freestanding cellular-structured GFs, as illustrated in **Figure 8c**. The GF/PEDOT:PSS composites possess an enhanced electrical conductivity from 11.8 to 43.2 S/cm after the incorporation of PEDOT:PSS. The modified grapheme foam with a density of 18.2×10^{-3} g/cm^3 provide a remarkable EMI SE of 91.9 dB (identified as SE_T in **Figure 8d**).

3.2.5 Graphene aerogels

Aerogel is a synthetic porous ultralight material derived from a gel, in which the liquid component used in gel are replaced by air. In recent years, the great potential of graphene aerogel (GAs) in EMI shielding applications has been confirmed by several researchers. Song et al. [36] reported that the EMI SE of GA-carbon textile hybrid with a thickness of 2 mm was 27 dB. The 3D scaffold GA greatly enhances
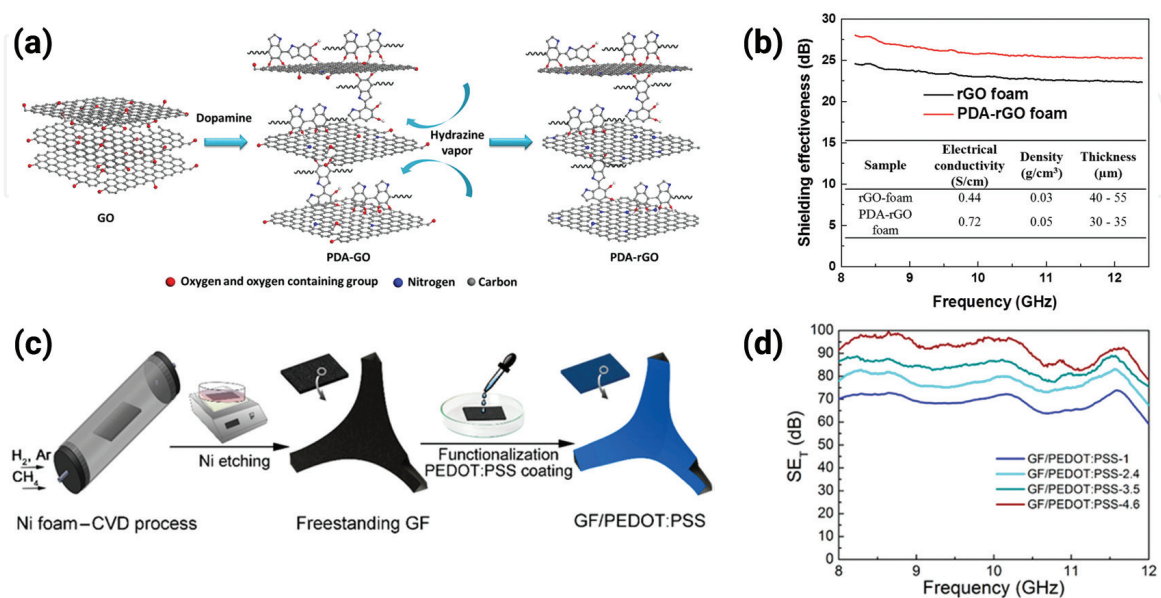

Figure 8.
(a) Schematic representation of the preparation of PDA-GO and PDA-rGO; (b) EMI SE of rGO foam and PDA-rGO foam [34]; (c) schematic procedure of the preparation of GF/PEDOT:PSS composites; (d) EMI SE of GF/PEDOT:PSS composites as a function frequency [35].

the conductive network while maintaining the advantage of light carbon textile. Singh et al. [37] studied the EMI SE of pure GA, which was 20 dB, with a density ~75 mg /cm³ and a thickness of 2 mm. They discussed the EMI shielding mechanism by correlating the EM wave interaction with the 3D porous structure. Zeng et al. [38] fabricated an ultralight and highly elastic rGO/lignin-derived carbon (LDC) composite aerogel with aligned microspores and cell walls by directional freeze-drying and carbonization method. The EMI SE of rGO/LDC composite aerogels with a thickness of 2 mm could reach up to 49.2 and 21.3 dB under ultralow densities of 8.0 and 2.0 mg/cm³, respectively.

The graphitization of GAs facilitates to improve its electrical conductivity, thus improving the EMI SE. Liu et al. [39] reported an effective method of manufacturing an integrated graphene aerogel (IGA) using a complete bridge between rGO sheets and polyimide macromolecules via graphitization at 2800°C, as shown in **Figure 9a**. The rGO sheets were efficiently reduced to graphene during graphitization, while the polyimide component was graphitized to turbostratic carbon to connect the graphene sheets, resulting in a high EMI SE of ~83 dB in X-band at a low density of 18 mg/cm³, as shown in **Figure 9b**. The EMI shielding mechanism analysis for the porous IGA revealed that most of the incident EM wave was dissipated through absorption, thus forming an absorption-dominant EMI shielding mechanism.

Different reduction process of graphene oxide (GO), including chemical reduction and thermal reduction would affect the EMI shielding performance of GAs. Bi et al. [40, 41] carried out a comprehensive study of EMI shielding mechanisms of GAs solely consisted of graphene sheets to determine the main parameters of high EMI SE. As shown in **Figure 10a**, two types of ultralight (4.5–5.5 mg/cm³) 3D GAs were prepared by chemical reduction and thermal reduction of GO aerogels. The EMI SE reached 27.6 and 40.2 dB for chemically reduced graphene aerogel (GAC) and thermally reduced graphene aerogel (GAT), respectively. The distinct graphene surface resulted from different processing pathway led to different EM wave
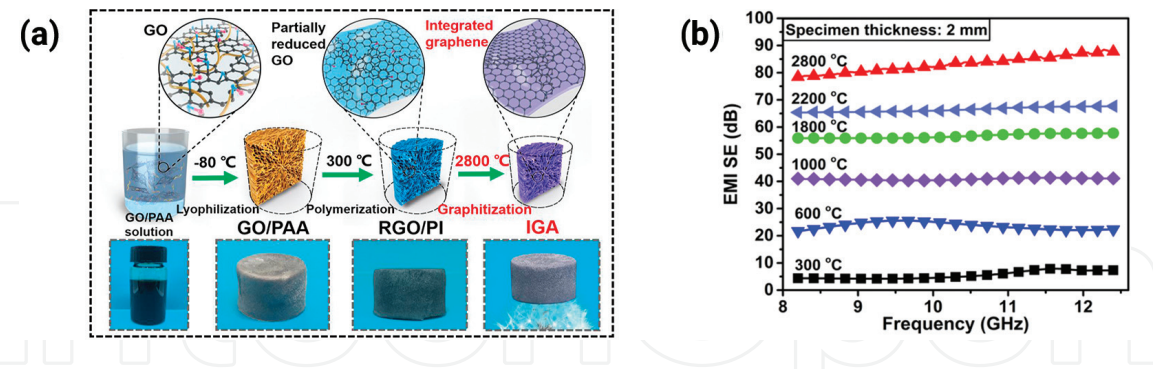

Figure 9.
(a) Schematic illustration for fabricating IGA and (b) effect of annealing temperature on EMI shielding performance of IGAs [39].
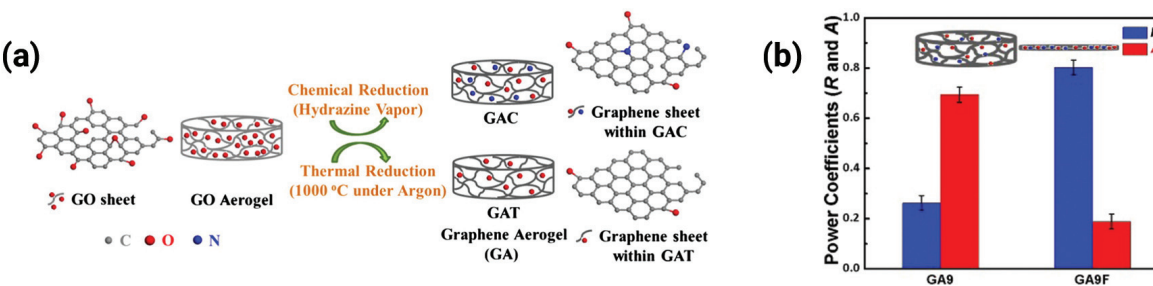

Figure 10.
(a) Schematic representation of the preparation process of GAC and GAT [42] and (b) R & A of GA9 and GA9F [41].

response upon striking the graphene/air interface. Nitrogen-doping and side polar groups induced strong polarization effects in GAC. Higher extent of reduction of the grapheme sheets in GAT left a smaller amount of side polar groups and formed more sp^2 graphitic lattice, both favored π-π stacking between the adjacent graphene sheets. The enhanced polarization effects and the increased electrical conductivity of GAT contributed to better EMI shielding performance. Bi further investigated the effect of porosity on EMI shielding mechanisms compressing the aerogel (GA9) into thin film (GA9F), as shown in **Figure 10b**. The highly connected conducting network resulted in a significant increase in the electrical conductivity of GA9F, while the EMI SE remained unchanged at constant rGO content. The observation was contradictory to the previous outcomes that higher electrical conductivity or better-connected network contributed to higher EMI SE. Hence, the fact can be believed that the EMI SE is highly dependent on the effective amounts of materials response to the EM waves. Despite the similar intrinsic properties of rGO, the amount of absorption of EM waves in GA9 was much higher than that in GA9F when the EM waves penetrated through the porous structure. The cavities within the highly porous GA absorbed the EM waves through multiple internal reflections and eventually depleted the energy. Hence, the tightly connected conducting network within GA9F changed the EMI shielding mechanism from absorption to reflection.

4. Conclusions

Generally, EMI shielding is defined as the prevention of the propagation of EM waves from one region to another by using shield materials. With the development of electronic industry, weight reduction is an additional technical requirement besides the good EMI shielding performance. Metal as a traditional EMI shielding material has been replacing with lighter materials, such as polymer-based composites, foams and aerogels. This chapter reviewed various types of lightweight materials with their EMI SEs corresponding to their EMI shielding mechanisms. To verify the benefits of using lightweight materials for EMI shielding applications, a comprehensive comparison was performed as shown in **Figure 11**. All the data in **Figure 11** were collected from the
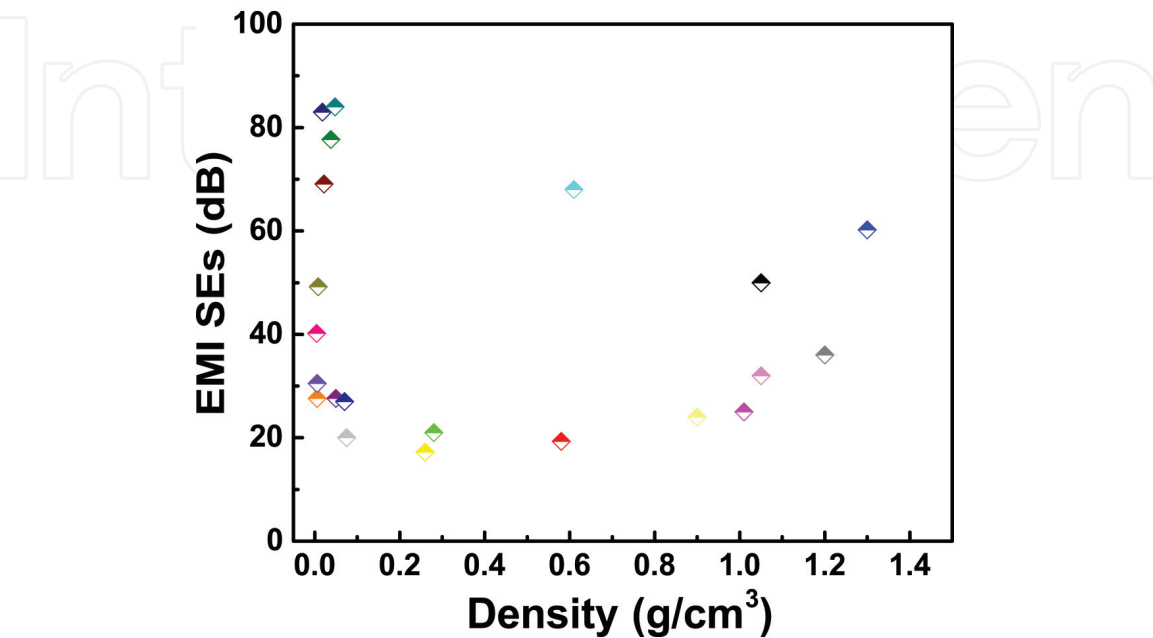

Figure 11.
Comparison of EMI SEs of lightweight materials as a function of density of materials.

reference papers listed in this chapter. Although the data are not involved all the published results, they are representative to the library of lightweight EMI shielding materials. The reported EMI SEs of polymer-based composites containing conductive fillers varied in the range of 20–60 dB corresponding to the densities higher than 0.8 g/cm^3. Polymer-based foams reinforced with additional conductive fillers and carbon foams outperform polymer-based composites in terms of EMI SE. They possessed comparable EMI SE of 20–80 dB with the lower density (<0.8 g/cm^3). Aerogels with ultralow densities (<100 mg/cm^3) exhibited high EMI SEs in the same range of polymer- and carbon-based foams, indicating they can be used as an ideal potential lightweight EMI shielding materials though the mechanical properties of aerogels still remain a big issue.

Acknowledgements

Conflict of interest

No conflict of interest.

Author details

Liying Zhang[1*†], Shuguang Bi[2†] and Ming Liu[3]

1 Center for Civil Aviation Composites, Donghua University, Shanghai, China

2 Chemistry and Chemical Engineering College, Wuhan Textile University, Wuhan, China

3 Temasek Laboratories, Nanyang Technological University, Singapore

*Address all correspondence to: lyzhang@dhu.edu.cn

†These authors contributed equally to this work.

IntechOpen

References

[1] Davidovits J. 30 years of successes and failures in geopolymer applications. Market trends and potential breakthroughs. In: Geopolymer Conference; 2002; Melbourne, Australia

[2] Perez R. Handbook of Electromagnetic Compatibility. London, United Kingdom: Academic Press; 1995

[3] Thomassin J-M, Jerome C, Pardoen T, Bailly C, Huynen I, Detrembleur C. Polymer/carbon based composites as electromagnetic interference (EMI) shielding materials. Materials Science & Engineering R-Reports. 2013;**74**:211-232

[4] Yang YL, Gupta MC. Novel carbon nanotube-polystyrene foam composites for electromagnetic interference shielding. Nano Letters. 2005;**5**: 2131-2134

[5] Crooks LE. Noise reduction techniques in electronic systems (2nd ed.), Henry W. Ott. Wiley-Interscience: New York. 1988. Magnetic Resonance in Medicine. 1989;**10**:426-427

[6] Al-Saleh MH, Sundararaj U. Electromagnetic interference shielding mechanisms of CNT/polymer composites. Carbon. 2009;**47**:1738-1746

[7] Chung DDL. Electromagnetic interference shielding effectiveness of carbon materials. Carbon. 2001;**39**: 279-285

[8] Paul CR. Introduction to Electromagnetic Compatibility. 2nd ed. New York, United States: John Wiley & Sons, Inc; 2006

[9] Sihvola A. Electromagnetic Mixing Formulas and Applications. London, United Kingdom: Institution of Engineering and Technology; 1999

[10] Koledintseva M, Ravva PC, DuBroff R, Drewniak J, Rozanov K, Archambeault B; Ieee. Engineering of composite media for shields at microwave frequencies. In: EMC 2005: IEEE International Symposium on Electromagnetic Compatibility. Proceedings. Vols. 1-3. 2005. pp. 169-174

[11] Chen C-S, Chen W-R, Chen S-C, Chien R-D. Optimum injection molding processing condition on EMI shielding effectiveness of stainless steel fiber filled polycarbonate composite. International Communications in Heat and Mass Transfer. 2008;**35**:744-749

[12] Shyr T-W, Shie J-W. Electromagnetic shielding mechanisms using soft magnetic stainless steel fiber enabled polyester textiles. Journal of Magnetism and Magnetic Materials. 2012;**324**:4127-4132

[13] Kim MS, Kim HK, Byun SW, Jeong SH, Hong YK, Joo JS, et al. PET fabric/polypyrrole composite with high electrical conductivity for EMI shielding. Synthetic Metals. 2002;**126**: 233-239

[14] Lakshmi K, John H, Mathew KT, Joseph R, George KE. Microwave absorption, reflection and EMI shielding of PU-PANI composite. Acta Materialia. 2009;**57**:371-375

[15] Courric S, Tran VH. The electromagnetic properties of poly (p-phenylene-vinylene) derivatives. Polymer. 1998;**39**:2399-2408

[16] Courric S, Tran VH. The electromagnetic properties of blends of poly (p-phenylene-vinylene) derivatives. Polymers for Advanced Technologies. 2000;**11**:273-279

[17] Taka T. EMI shielding measurements on poly(3-octyl-thiophene) blends. Synthetic Metals. 1991;**41**:1177-1180

[18] Sanchez-Gonzalez J, Macias-Garcia A, Alexandre-Franco MF, Gomez-Serrano V. Electrical conductivity of carbon blacks under compression. Carbon. 2005;**43**:741-747

[19] Al-Saleh MH, Sundararaj U. A review of vapor grown carbon nanofiber/polymer conductive composites. Carbon. 2009;**47**:2-22

[20] Tibbetts GG, Lake ML, Strong KL, Rice BP. A review of the fabrication and properties of vapor-grown carbon nanofiber/polymer composites. Composites Science and Technology. 2007;**67**:1709-1718

[21] Iijima S, Ichihashi T. Single-shell carbon nanotubes of 1-nm diameter. Nature. 1993;**363**:603

[22] Iijima S. Helical microtubules of graphitic carbon. Nature. 1991;**354**:56

[23] Geim AK, Novoselov KS. The rise of graphene. Nature Materials. 2007;**6**:183

[24] Nazir A, Yu H, Wang L, Haroon M, Ullah RS, Fahad S, et al. Recent progress in the modification of carbon materials and their application in composites for electromagnetic interference shielding. Journal of Materials Science. 2018;**53**:8699-8719

[25] Al-Saleh MH, Saadeh WH, Sundararaj U. EMI shielding effectiveness of carbon based nanostructured polymeric materials: A comparative study. Carbon. 2013;**60**:146-156

[26] Kim B-J, Bae K-M, Lee YS, An K-H, Park S-J. EMI shielding behaviors of Ni-coated MWCNTs-filled epoxy matrix nanocomposites. Surface & Coatings Technology. 2014;**242**:125-131

[27] Yim Y-J, Rhee KY, Park S-J. Electromagnetic interference shielding effectiveness of nickel-plated MWCNTs/high-density polyethylene composites. Composites Part B-Engineering. 2016;**98**:120-125

[28] Yang YL, Gupta MC, Dudley KL, Lawrence RW. Conductive carbon nanoriber-polymer foam structures. Advanced Materials. 2005;**17**:1999

[29] Zhang L, Wang LB, See KY, Ma J. Effect of carbon nanofiber reinforcement on electromagnetic interference shielding effectiveness of syntactic foam. Journal of Materials Science. 2013;**48**:7757-7763

[30] Zhang L, Roy S, Chen Y, Chua EK, See KY, Hu X, et al. Mussel-inspired polydopamine coated hollow carbon microspheres, a novel versatile filler for fabrication of high performance syntactic foams. ACS Applied Materials & Interfaces. 2014;**6**:18644-18652

[31] Xu Y, Li Y, Hua W, Zhang A, Bao J. Light-weight silver plating foam and carbon nanotube hybridized epoxy composite foams with exceptional conductivity and electromagnetic shielding property. ACS Applied Materials & Interfaces. 2016;**8**:24131-24142

[32] Zhang L, Liu M, Roy S, Chu EK, See KY, Hu X. Phthalonitrile-based carbon foam with high specific mechanical strength and superior electromagnetic interference shielding performance. ACS Applied Materials & Interfaces. 2016;**8**:7422-7430

[33] Lu D, Mo Z, Liang B, Yang L, He Z, Zhu H, et al. Flexible, lightweight carbon nanotube sponges and composites for high-performance electromagnetic interference shielding. Carbon. 2018;**133**:457-463

[34] Zhang L, Liu M, Bi S, Yang L, Roy S, Tang X-Z, et al. Polydopamine decoration on 3D graphene foam and its electromagnetic interference shielding properties. Journal of Colloid and Interface Science. 2017;**493**:327-333

[35] Wu Y, Wang Z, Liu X, Shen X, Zheng Q, Xue Q, et al. Ultralight graphene foam/conductive polymer composites for exceptional electromagnetic interference shielding. ACS Applied Materials & Interfaces. 2017;**9**:9059-9069

[36] Song W-L, Guan X-T, Fan L-Z, Cao W-Q, Wang C-Y, Cao M-S. Tuning three-dimensional textures with graphene aerogels for ultra-light flexible graphene/texture composites of effective electromagnetic shielding. Carbon. 2015;**93**:151-160

[37] Singh S, Tripathi P, Bhatnagar A, Patel CRP, Singh AP, Dhawan SK, et al. A highly porous, light weight 3D sponge like graphene aerogel for electromagnetic interference shielding applications. RSC Advances. 2015;**5**: 107083-107087

[38] Zeng Z, Wang C, Zhang Y, Wang P, Shahabadi SIS, Pei Y, et al. Ultralight and highly elastic graphene/lignin-derived carbon nanocomposite aerogels with ultrahigh electromagnetic interference shielding performance. ACS Applied Materials & Interfaces. 2018;**10**:8205-8213

[39] Liu J, Liu Y, Zhang H-B, Dai Y, Liu Z, Yu Z-Z. Superelastic and multifunctional graphene-based aerogels by interfacial reinforcement with graphitized carbon at high temperatures. Carbon. 2018;**132**:95-103

[40] Bi S, Zhang L, Mu C, Lee HY, Cheah JW, Chua EK, et al. A comparative study on electromagnetic interference shielding behaviors of chemically reduced and thermally reduced graphene aerogels.
Journal of Colloid and Interface Science. 2017;**492**:112-118

[41] Bi S, Zhang L, Mu C, Liu M, Hu X. Electromagnetic interference shielding properties and mechanisms of chemically reduced graphene aerogels.

Applied Surface Science. 2017;**412**: 529-536

[42] Bi S, Zhang L, Mu C, Lee HY, Cheah JW, Chua EK, et al. A comparative study on electromagnetic interference shielding behaviors of chemically reduced and thermally reduced graphene aerogels. Journal of Colloid and Interface Science. 2017;**492**:112-118